Original Research

Aging and chromatoid body assembly: Are these two physiological events linked?

Elisa G Santos[1], Maraisa A Silva[2], Renata P Amorim[1], Leticia de Souza Giordano[2], Dayana de Sales Silva[3], Lucas T Rasmussen[1,2,3] and Rita L Peruquetti[1,2,3]

[1]Office of the Associate Dean of Graduate Studies and Research, Sagrado Coração University (USC), Bauru, São Paulo 17011-160, Brazil; [2]School of Health Sciences, Sagrado Coração University (USC), Bauru, São Paulo 17011-160, Brazil; [3]Molecular Biology and Cytogenetics Laboratory, Sagrado Coração University (USC), Bauru, São Paulo 17011-160, Brazil
Corresponding author: Rita L Peruquetti. Email: rita.peruquetti@usc.br

Impact statement

The results discussed in this paper indicate that aging compromises the structure and physiology of chromatoid bodies (CBs) in post-meiotic male cells. Since CB is a fundamental structure for the differentiation of the mature male germ cell it is possible that this imbalance in CB physiology may play a role in the reduction of fertility in older men. It is important to note that not only the classic CB markers (such as the MIWI and MVH proteins) were used to showcase the structural changes in the CBs but also the main components of circadian cycle control (the CLOCK and BMAL1 proteins), indicating that the reduction of circadian control in aged males may contribute to these changes in CBs as well. Therefore, it is intriguing to evaluate the hypothesis that controlling these physiological/structural changes in CBs may be a way of delaying the effects of aging in males.

Abstract

The chromatoid body is a cytoplasmic male germ cell structure that plays a role in the regulation of mRNA transcription during spermatogenesis. A proteomic analysis of this structure has identified the presence of its classic molecular markers (MVH and MIWI), as well as a significant number of transient proteins. Circadian locomotor output cycles protein kaput (CLOCK) and brain and muscle ARNT-like 1 (BMAL1), which are molecular components of the circadian clock, are likely located in the chromatoid body in a transient fashion. This study sought to determine whether aging produces morphological changes in the chromatoid bodies of round spermatids similar to those previously observed in BMAL1 knockout mice. A sample of 30 male mice was divided into three groups: juvenile mice (45 days old), adult mice (120 days old), and old mice (+180 days old). Aging was confirmed by viability and sperm count analyses and testosterone dosage. Squash slides prepared with fragments of seminiferous tubules were immunostained for MVH, MIWI, BMAL1, and CLOCK detection. In juvenile and adult specimens, single round chromatoid bodies were observed using MVH/BMAL1 and MIWI/CLOCK immunostaining. In old specimens, many chromatoid bodies displayed changes in number and morphology, as well as an increase in the interactions between MVH and BMAL1; MIWI and CLOCK. Changes in chromatoid body morphology increased interactions between the proteins analyzed herein, and decreased amounts of these proteins in seminiferous tubules of older mice may indicate that aging influences the assembly and physiology of chromatoid bodies, which may, in turn, affect fertility.

Keywords: Aging, fertility, spermatogenesis, chromatoid body

Experimental Biology and Medicine **2018; 243: 917–925. DOI: 10.1177/1535370218784871**

Introduction

Aging is a complex process that involves social, economic, and biological factors.[1] The world's population is aging quickly and disproportionately. In 2005, there were approximately 670 million people aged 60 years or older on the planet, which represented 10% of the world's population. The United Nations (UN) estimates that, by 2050, this number will increase to approximately 2 billion people.[2]

Genetic factors associated with lower susceptibility to cognitive and degenerative disorders (such as Alzheimer's), more effective DNA repair processes, consistent size and quality of telomeres, the genetic makeup of mitochondrial DNA, and other traits have been reported as keys to longer life expectancy and better quality of life.[3]

Long non-coding RNAs (lncRNAs) also play important roles in the control of a wide array of biological processes that, when unbalanced, can cause age-related diseases such as cancer, cardiovascular diseases, and neurodegenerative diseases.[4,5]

Physiologically, the main changes associated with advanced age are changes in hormone levels (examples include estrogen, androgen, growth hormone/insulin-like growth factor), metabolic changes affecting nutrient utilization, and declines in fertility and the consequent decline in arousal and the rate of sexual behaviors.[6] Reduced metabolism rates in aged animals are deeply influenced by a change in the circadian rhythm, which has as key controllers the brain and muscle ARNT-like 1 protein (BMAL1) and the locomotor output cycles kaput protein (CLOCK).[7]

Although aging is known to contribute to a decrease in endocrine function in males and to reduce the quality of some semen parameters, the spermatogenesis process continues for years in the absence of pathological factors.[8] An important cytoplasmic structure typical of male germ cells and essential for spermatozoid maturation is known as the chromatoid body (CB).[9–12]

The CB is an irregularly shaped cytoplasmic granule that can be found in the cytoplasm of initial spermatids as a single granule.[13] Evidence suggests that the CB plays a role in regulating mRNA transcription during spermatogenesis and participates in the control of gene expression through the action of a series of small non-coding RNAs: miRNA and PIWI-interacting RNA, or piRNA.[14] Studies have shown that this mRNA metabolism, which is mediated by small non-coding RNAs and executed by the CB, is crucial for the spermatogenesis process to progress correctly and for the formation of mature male reproductive cells.[15–17]

Studies from this field of research have attempted to describe the full protein and transcriptome composition of the CB in order to identify all of the pathways through which this structure contributes to the control of sperm cell differentiation. Meikar *et al.*[18] were able to identify the complete protein and RNA content inside this macromolecular complex. This analysis confirmed the proteins known as CB markers: mouse VASA homologue (MVH), mouse Argonaute/PIWI family RNA-binding proteins (MIWI), which are the most abundant elements in the molecular makeup of CBs. However, the same authors also identified a very representative quantity of proteins exhibiting nuclear locations/functions and temporarily residing in the CB.[18]

Based on an analysis of CB formation during spermatogenesis in BMAL1 knockout (KO) mice, which exhibit the early onset of aging-associated phenotypes and infertility (among other traits), Peruquetti *et al.*[19] report the presence of both of the proteins central to the control of circadian rhythms (CLOCK and BMAL1) in the molecular composition of the CB; they also report that animals in which BMAL1 protein expression was blocked exhibited CBs with many morphological abnormalities (such as changes in size, number, and shape). However, the precise biological significance of the location of CLOCK and BMAL1 in the CBs of post-meiotic cells has not yet been determined. Additionally, BMAL1 KO male exhibit many copulatory defects, demonstrating the importance of the BMAL1 protein in the maintenance of neural circuits that drive pheromone-mediated mating behaviors.[20]

Because the increase in the life expectancy of the world's population and decreases in fertility are resulting in an aging human population on the planet, the objective of this study was to determine whether natural physiological aging produces structural changes to the CBs of round spermatids and how this event may be associated with decreases in fertility. The results obtained in this study may serve as the foundation for discussions on how to address the issue of an aging human population in the world today.

Materials and methods

In this study, 30 male Swiss mice (*Mus musculus*) were used. The animals were grouped according to their age: 10 45-day-old mice (the juvenile group); 10 120-day-old mice (the adult group); and 10 mice older than 180 days (the old group). They were supplied by the vivarium of Sagrado Coração University (USC) in São Paulo State, Brazil. During the experiments, the animals were cared for in accordance with Brazilian Animal Welfare Regulations, which is monitored by the Brazilian National Council to Control Animal Experimentation (CONCEA). The animals were kept in cages with food and water offered *ad libitum*, at a controlled temperature (between 21°C and 25°C), and with a 12:12-h light:dark cycle. For biological material collection, the animals were euthanized through the injection of barbiturates followed by cervical dislocation. All of the procedures used for euthanasia are consistent with the CONCEA Euthanasia Practice Guidelines.[21] This study was approved by the Ethics Committee for Animal Experimentation of Sagrado Coração University (CEUA/USC) under protocol numbers 1192290515 and 7445240415.

Experimental design

Most of the mice used in this study were from the same litter, though some were from different litters born within the same time frame. The mice were randomly grouped together and were raised until euthanasia at specific ages: 45 days, 120 days, or more than 180 days. After each animal was euthanized, one of its testicles was immediately processed: the seminiferous tubules were separated by their stages in the spermatogenic cycle and were then used in the squash slide preparation and the immunofluorescence analysis. The other testicle was removed from the scrotum, decapsulated, stored in a microtube, and frozen in liquid nitrogen for subsequent use in daily spermatozoid production (DSP) counts as well as for total protein extraction. The epididymis were collected, stored in microtubes, and frozen in liquid nitrogen for the subsequent sperm viability analysis. Blood samples were collected from the chest cavity and the cavities of the heart using 1 mL syringes and were immediately processed to determine serum testosterone levels.

Determining DSP

The seminiferous tubules of the animals in each age group were thawed individually at the time of use. The seminiferous tubules were weighed and then diluted in an STM solution (0.9% NaCl/0.05% Triton X100). Two Neubauer chambers were prepared for each animal using 1 μL of the seminiferous tubules homogenate diluted in 99 μL of STM (1:10). In each chamber, the number of spermatozoids was counted in five fields (the four extremities and the center). After the average number of spermatozoids in the 4 positions in the chamber was determined, DSP was calculated following the procedure provided by Robb *et al.*[22] and Garcia *et al.*[23]

Viability of spermatozoids in the epididymis

As part of the spermatozoid viability analysis, the epididymis of each animal from each experimental group was thawed separately. Each Petri dish received 1 mL of 0.1% BSA/PBS1× at 37°C in order to form a drop in the center of the dish. Next, one epididymis was placed on this drop at a time. Using a stereoscopic microscope, the head of the epididymis was perforated by a needle in order to allow for the release of the seminal fluid. The seminal fluid was then homogenized with a 0.1% BSA/PBS1× solution. Next, 100 μL of this homogenate was collected and then added to 100 μL of eosin dye. This mixture was used to prepare the smear on a slide, and 100 spermatozoids per slide were analyzed. In this analysis, both inviable spermatozoids (those whose heads were stained by the eosin dye) and viable spermatozoids (those whose heads were not stained by the eosin dye) were counted. These preparations were adapted based on the technique proposed by Bjorndahl *et al.*[24]

Plasma testosterone levels

Approximately 0.5 mL of blood was collected from the chest cavities and cavities of the heart soon after the animals were euthanized. Blood was collected in microtubes and stored at room temperature for approximately 1 h. The serum was separated from the whole blood using centrifugation at 5000 r/min for 15 min at 4°C. The serum was collected in new tubes, which were immediately frozen in liquid nitrogen and kept at −80°C until dosing. Serum testosterone levels were measured using the Abbot Architect *ci*8200 based on human dosages.

Immunofluorescence in squash preparations

After the seminiferous tubules were obtained, they were separated by spermatogenic cycle stage, which was determined via observation under a transilluminating dissection microscope.[25] The slides containing the squash preparations of seminiferous tubules in stages IV–VI of the spermatogenic cycle were immersed in a 4% PFA/PBS solution in ice for 10 min. Next, the slides were washed in PBS and then immersed in 0.2% Triton-X100/PBS at room temperature for 5 min. Non-specific staining was blocked using 5% BSA/PBS for 1 h at room temperature. After the blocking process, the samples were incubated overnight at 4°C with the following primary antibodies: PIWIL1 (N-17): sc-22685 (1:100); CLOCK: (C-276): sc-25–36 (1:100); BMAL1: (H-170): sc-48790 (1:100) (Santa Cruz Biotechnology, Inc. – S-19); and αDDX4 (MVH): Ab27591 (1:100) (Abcam). After incubation, the slides were washed in PBST. The secondary antibodies of interest, which were conjugated with different fluorescent agents (Alexa Fluor® 594 Chicken Anti-Goat IgG [H + L] (1:200), Alexa Fluor® 488 Goat Anti-Mouse (1:200), Alexa Fluor® 532 Goat Anti-Mouse (1:200), and Alexa Fluor® 488 Goat Anti-Rabbit) (1:200), were diluted in 5% BSA/PBS and incubated for 1 h at room temperature. Slides labeling followed two distinct systematics: (a) Slides were incubated with each of the primary antibodies alone (PIWIL1; CLOCK; BMAL1; and MVH), followed by incubation with the two secondary antibodies of interest to check for crosslinks between the primary and secondary antibodies. (b) No cross-reaction was detected between any of the primary antibodies with their nonspecific secondary antibodies. Detection of overlap between MVH and BMAL1 as well as between MIWI and CLOCK was performed separately by simultaneous incubation of these primary antibodies with their respective secondary antibodies.

The slides were washed again in PBST, and the material was then stained with a DAPI solution to display the nuclei. Finally, the slides were washed in PBS, mounted with Ultra Cruz Mounting Medium: sc-24941 (Santa Cruz Biotechnology, Inc.), and analyzed under a fluorescent microscope (Nikon Eclipse 80i, Nikon Instruments, Inc.) attached to a QImaging MicroPublisher 3.3 cooled camera with RTV for determination of Pearson's Coefficient (Rr). Laser confocal microscope (Leica TCS SPE, with Leica Application Suíte – Advanced Fluorescence (LAS AF) version 2.7.3.9.723 1997–2012 Leica Microsystems) was used for photo documentation and qualitative analysis.

Co-localization analysis—Pearson's coefficient

The immunofluorescence images were collected using the Image-Pro® Plus software, version 5.1.2 for Windows XP. The co-localization between MVH/BMAL1 and between MIWI/CLOCK was tested in images from five different animals from each age group. Only initial spermatids with evident CB staining (MIWI or MVH) were used to determine Pearson's coefficient (Rr). The images with background staining were also excluded from the calculations. The co-localization coefficient or Pearson's coefficient (Rr = 1) was calculated using the same image-capturing software.

Total protein extraction and immunoblot

Seminiferous tubules were homogenized in 500 μL of RIPA buffer containing inhibitors (1 M NaF, complete protease cocktail inhibitor, and 0.1 M PMSF). Next, the product was centrifuged at 14,000× *g* for 15 min at 4°C. The supernatant was removed after centrifugation. The total extracted proteins were quantified using a NanoDrop 2000

spectrophotometer (Thermo Scientific®). The proteins were diluted in RIPA buffer with inhibitors to homogenize the quantities. They were then diluted in Laemmli buffer and stored at −20°C until use.

For the immunoblot assay, approximately 25 μg of each protein extract pool (45 days old, 120 days old and +180 days old seminiferous tubules extracts) were separated in one single 10% SDS-polyacrylamide gel and transferred to a PVDF membrane using electroblotting. Next, the membranes were washed in PBST and incubated for 1 h at room temperature in 5% nonfat milk/PBST to block non-specific staining After incubation, the membranes were again washed in PBST and incubated with the PIWIL1 (N-17): sc-22685 (1:400); anti-CLOCK: (C-276): sc-25–36 (1:200); anti-BMAL1: (H-170) sc-48790 (1:100) (Santa Cruz Biotechnology, Inc. – S-19); αDDX4 (MVH): Ab27591 (1:1000) (Abcam); and anti-α-tubulin (T5168) (1:10,000) (Sigma Aldrich), all of which were diluted in 5% nonfat milk/PBST and incubated overnight at 4°C. Proteins of interest weights are: 75 KDa (MVH), 71 KDa (BMAL1), 95 KDa (CLOCK), and 98 KDa (MIWI). Control protein weight is 50 KDa (Tubulin). The membrane was cut into four pieces containing proteins of different sizes from the same gel for the detection of the following combination of proteins: (1) CLOCK and MVH (after stripping CLOCK signal); (2) MIWI and BMAL1 (after stripping MIWI signal); (3) tubulin for both combinations.

After incubation with the primary antibody, the membranes were again washed in PBST and were then incubated with secondary antibodies (HRP rabbit anti-mouse-Invitrogen 616520 (1:4000), HRP Goat anti-rabbit IgG: sc-2004 (1:5000); and HRP donkey anti-goat IgG: sc-2020) (1:500). The antibodies were diluted in 5% nonfat milk/PBST for 1 h at room temperature. Finally, the membranes were washed in PBST, dried, and imaged.

To determine the relative amount of each protein in each group, band sizes were measured using the Image J program – Image Processing and Analysis in Java, Version 1.51e (http://rsb.info.nih.gov/ij/). Measures were considered after performing five different Western blot assays following the same systematic as described above.

Statistical analysis

The normality of all of the data was tested. Each result obtained from each group was obtained using the Kruskal–Wallis ANOVA test within the Statsoft Inc. software (2011) and the Statistica data analysis software system, version 10. The statistical analyses were based on Zar,[26] and the difference was considered significant when $P < 0.05$.

Results

Analysis of the general reproductive parameters

Some general reproductive parameters, such as DSP, sperm viability, and plasma testosterone levels, were measured and compared to expected parameters for each age group in order to determine the aging-associated phenotype in the model used in this study.

Table 1. Daily spermatozoa production ratio (DSPr) of each age group in order to determine the aging-associated phenotype in the model used in this study.

Age	Daily spermatozoa production (DSPr×10^6) Mean±SD	Kruskal–Wallis ANOVA
45 days old (*n*=5)	39.2221±6.47a	*P*=0.015
120 days old (*n*=6)	42.7811±10.74a	
+180 days old (*n*=5)	14.3808±1.56b	

Note: Different letters (a,b) indicate statistical difference.

Table 2. Counting of viable and unviable spermatozoa in the epididymis of each age group in order to determine the aging-associated phenotype in the model used in this study.

Age	Spermatozoa in the epididymis	
	Viable (*n*) Mean±SD	Unviable (*n*) Mean±SD
45 days old (*n*=5)	63.75±6.23	40.5±6.75
120 days old (*n*=5)	63.75±3.86	40.5±7.13
+180 days old (*n*=5)	60.75±5.90	43.5±4.93
Kruskal–Wallis ANOVA	*P*=0.776	*P*=0.185

Note: No statistical difference was detected.

Table 3. Plasma testosterone levels of each age group in order to determine the aging-associated phenotype in the model used in this study.

Age	Testosterone levels (ng/dL) Mean±SD	Kruskal–Wallis ANOVA
45 days old (*n*=5)	1032.608± 34.47a	*P*=0.024
120 days old (*n*=5)	1865.050±1273.56b	
+180 days old (*n*=5)	1094.510±1586.12a,b	

Note: Different letters (a,b) indicate statistical difference.

A significant drop in DSP was observed in the oldest age group (Table 1). Despite this reduction in DSP, germ cell quality was not affected in the oldest group: the number of viable and inviable spermatozoid remained the same among the three different age groups analyzed (Table 2). When plasma testosterone levels were compared among the three ages, higher levels were observed in the adult animals relative to the juveniles; a slight drop was also observed in the older group, which reached levels comparable to those of the juveniles (Table 3).

Analysis of the numerical and morphological organization of CBs in round spermatids

Slides containing squash preparations of seminiferous tubules in stages IV–VI of the spermatogenic cycle underwent individual labeling with the MVH, MIWI, CLOCK, and BMAL1 proteins; immunofluorescence was used to detect the isolated distribution of each of these proteins in round spermatids (Figures 1 and 2). Double labeling was also performed to determine co-localization of the MVH and BMAL1 proteins (Figure 1) and of the MIWI and

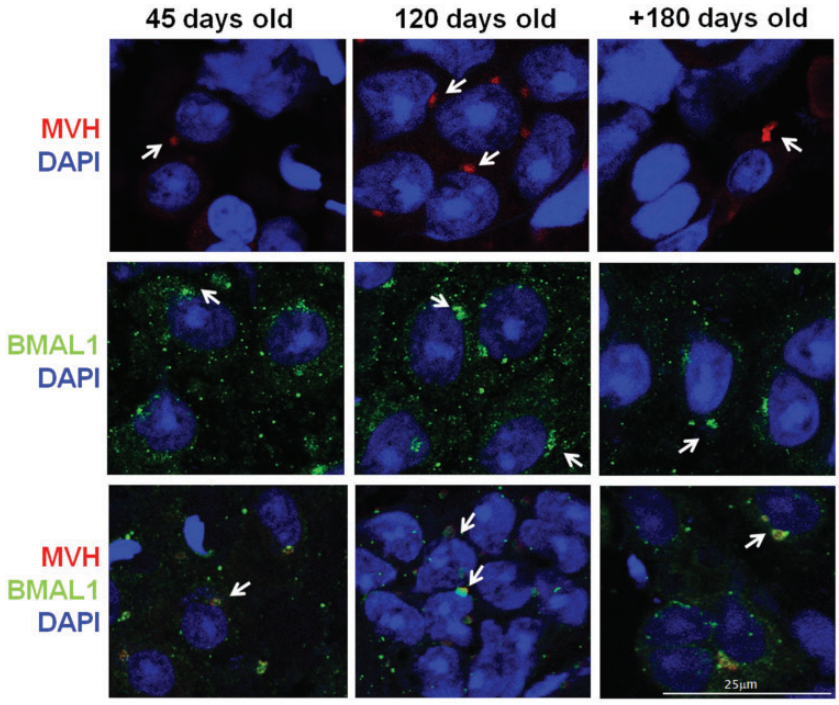

Figure 1. Detection of the expression of MVH, BMAL1, and overlap between MVH/BMAL1 proteins by immunofluorescence in seminiferous tubules at stages IV–VI of the spermatogenic cycle of each age group. Arrows: CBs. (A color version of this figure is available in the online journal.)

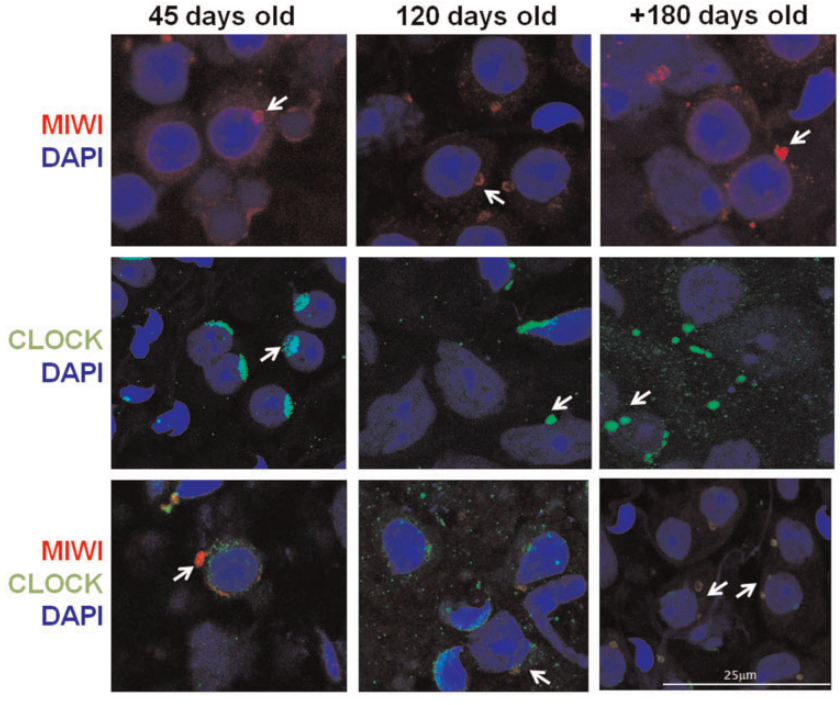

Figure 2. Detection of the expression of MIWI, CLOCK, and overlap between MIWI/CLOCK proteins by immunofluorescence in seminiferous tubules at stages IV–VI of the spermatogenic cycle of each age group. Arrows: CBs. (A color version of this figure is available in the online journal.)

CLOCK proteins (Figure 2). All of the proteins with exception of CLOCK in juvenile samples were located in the CBs of round spermatids, which were displayed as individual structures typically round in shape and located close to the nucleus of the cell in both juvenile and adult animals (Figures 1 and 2). In older animals, however, the CB was frequently found to be fragmented or with multiple markings. The signals also revealed abnormalities in CB morphology, such as irregular shapes (Figures 1 and 2).

Pearson's coefficient, which is one index used to define the degree of overlap between two or more markings, was applied to the slides with double markings (MVH/BMAL1 and MIWI/CLOCK). Higher overlap was found between the MVH and BMAL1 proteins in round spermatids from older animals relative to the adults, and higher overlap was also observed between the MIWI and CLOCK proteins in round spermatids from older animals relative to juveniles (Table 4). The lowest Rr value was found in the overlap between MIWI and CLOCK in CBs of juvenile round spermatids, which could also be seen at Figure 2.

CB maker and circadian protein expression in seminiferous tubules

A pool of total extracted proteins from the testicle of animals at different ages (juveniles, adults, and old mice) was used to detect expression and to quantify BMAL1, MVH, CLOCK, MIWI, and tubulin using Western blot (Figure 3).

When the proteins were quantified in each age group, higher amounts of MVH, MIWI, and CLOCK proteins were found in the juvenile group relative to the adult group, and the lowest amounts were detected in the older animals (Figure 4). Meanwhile, quantities of BMAL1 gradually decreased as the animals aged, and the lowest levels were detected among the oldest animals (Figure 4). The relative amount of tubulin was used as a reaction control and did not vary in the comparison between the three groups (Figure 4).

Discussion

General reproductive parameters

DSP, spermatozoid viability in the epididymis, and serum testosterone levels were the reproductive parameters measured in this experiment in order to evaluate the natural aging process in the animals used. The oldest animals were found to exhibit the lowest amount of DSP relative to the juvenile and adult groups. However, there were no differences in spermatozoid viability in the epididymis among the three age groups tested. A review performed by Gunes *et al.*[27] showed that spermatozoid number and viability are parameters which are negatively correlated with aging.

Testosterone levels are associated with developmental stage: testosterone increases gradually as mammals reach sexual maturity and tends to decrease at more advanced ages or as a result of other factors, such as certain pathologies or exposure to endocrine disruptors.[28,29] In this study, higher serum testosterone levels were found in adult animals, and lower levels were found in the oldest animals than in the juvenile (immature) animals.

Natural aging process considered in this study was chosen based on results previously obtained in studies on BMAL1 KO mice[30]. BMAL1 KO male mice possess a phenotype associated with accelerated aging, exhibiting DSP levels reduced by approximately 70% as well as lower serum testosterone levels when compared to their BMAL1 WT controls.[30] In our study, we were able to mimic many of these BMAL1 KO phenotypic characteristics.

Expression, distribution, and co-localization of MVH/BMAL1 and MIWI/CLOCK proteins in CBs of round spermatids

The CBs of round spermatids from seminiferous tubules in stages IV–VI of the spermatogenic cycle of juvenile and

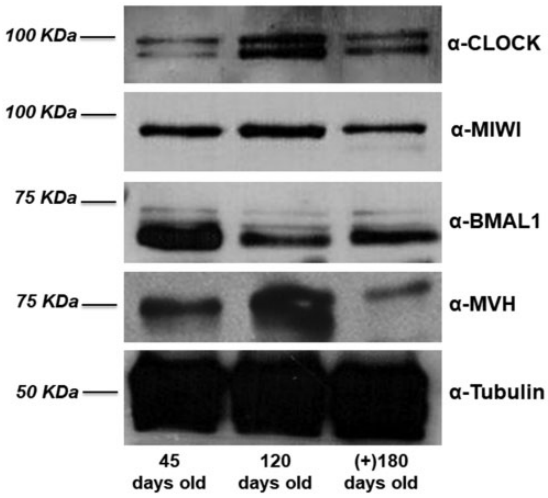

Figure 3. Immunoblot to detect the expression of CLOCK, MIWI, BMAL1, and MVH in a pool of total protein extracts from seminiferous tubules of each age group. Tubulin expression was used as reaction control.

Table 4. Pearson's correlation (Rr) of co-localization between MVH/BMAL1 and MIWI/CLOCK in round spermatids of each age group.

Assay	Age (days old)	Round spermatids (*n*)	Pearson's coefficient (Rr) Mean±SD	Kruskal–Wallis ANOVA
MVH/BMAL1	45	38	0.791±0.114a	*P*=0.000
	120	79	0.719±0.173a,b	
	+180	99	0.811±0.130a,c	
MIWI/CLOCK	45	25	0.229±0.136a	*P*=0.028
	120	34	0.288±0.182a,b	
	+180	24	0.363±0.166b	

Note: Analyses were performed by immunofluorescence detection in squash preparations of seminiferous tubules at stages IV–VI of the spermatogenic cycle. Different letters (a,b,c) indicate statistical difference.
BMAL1: brain and muscle ARNT-like 1; CLOCK: circadian locomotor output cycles protein kaput; MVH: mouse VASA homologue.

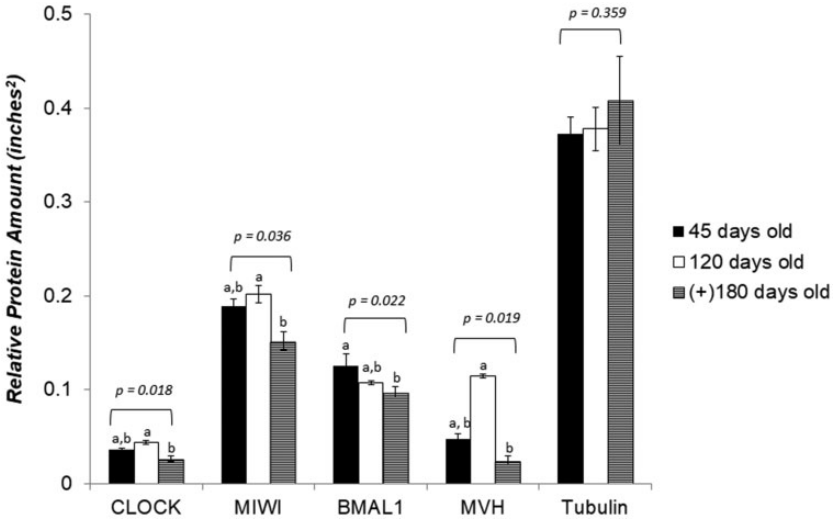

Figure 4. Relative amounts of CLOCK, MIWI, BMAL1, MVH, and tubulin detected by immunoblot of pool of total protein extracts from seminiferous tubules of each age group. Different letters (a,b) indicate statistical difference.

adult mice were detected using immunofluorescent labeling of the MVH, MIWI, BMAL1, and CLOCK proteins in association or in isolation. The CBs displayed as irregularly spherical, in isolation, and with relatively large markings (~1 μm) associated with the nuclear envelope. These observations coincide with the standard description of CBs from round spermatids in the literature, which reports that this structure is found as a solitary granule specifically in stages IV–VI of the spermatic cycle.[31,32]

However, the same type of preparation for older animals revealed CBs with different shape as well as the existence of multiple markings in a single round spermatid. The morphological and numerical changes described herein are consistent with the abnormalities described by Peruquetti *et al.*[19] in their analysis of CBs of round spermatids from BMAL1 KO mice. In their study, Peruquetti *et al.*[19] discuss whether these changes in the CBs found in BMAL1 KO mice were caused by the physiologically important location of BMAL1 in the CBs, or whether these changes are associated with the early onset of the aging-associated phenotype that these animals exhibit. Based on these observations, it can be concluded that the natural aging process may also lead to morphological or structural changes to the CBs of round spermatids.

In their review, de Mateo and Sassone-Corsi[33] also report that the CB may vary in quantity and morphology in other types of cells apart from round spermatids, as well as in seminiferous tubules in other stages of the spermatogenic cycle. This finding supports the argument that aging may compromise both the entire spermatogenesis process and the organization of seminiferous tubules.[8] These alterations in the dynamic of the general spermatogenesis may culminate in changes to this typical structure of male germ cells (the CB), which is crucial for the differentiation of spermatozoids.

Another important finding was that, despite the increase in the coefficient of overlap between the proteins analyzed in the oldest animals (MVH/BMAL1 and MIWI/CLOCK), the Western blot analyses detected a drop in overall expression of these proteins, particularly when the oldest mice were compared to the adult mice. Many authors have described the CB as a structure that possesses proteasome properties, or a center that includes degradation components where proteins and RNAs that are not used in the final processes of male germ cell differentiation are sent to be degraded.[34,35] Components involved in the intracellular trafficking network of autophagic vesicles have also been detected in the CB, a finding which indicates that the CB may be involved in autophagic activities occurring in germ cells undergoing differentiation.[36] When associated with the increased overlap of CLOCK and BMAL1 circadian proteins and specific components of the CB, the decreased expression of these proteins in the seminiferous tubules of the oldest animals may indicate that these proteins are being sent to the CB to be degraded, a process which would lead to a decrease in their expression. This evidence points to the possible involvement of components of circadian control in maintaining male fertility. It is known that drastic changes in the circadian clock or in the quantity or quality of the components that control this cycle are likely to be closely correlated with the development of certain pathologies, such as obesity, diabetes, reduced memory function, and sleep disorders, all of which do even greater damage at advanced ages.[7] Thus, the reduced expression of these proteins in germ cells, which is a physiological event inherent to aging, may also be associated with reduced physiological activity of male reproductive cell maturation.

In addition, the study by Woodland[37] sought to describe the importance of the development of sexual reproduction for the evolution of multicellularity in animals and found that the development of germ line cells, as well as of the structures exclusive to these cells (such as the CB), may contribute to organisms' life expectancy and ability to diminish or delay the effects of aging.

Because physiological aging is a process largely governed by the actions of lncRNAs[4,5] and of miRNAs,[38,39] it is possible that this process would negatively affect the structural organization of the CB, since its role in the

post-transcriptional control of major mRNAs (which must be transcribed in initial stages of spermatogenesis for protein synthesis later on this process) is largely based on the actions of small non-coding RNAs.[14,17]

In conclusion, or results reflect the physiological importance of maintaining the morphological integrity of CBs in round spermatids—not only to maintain reproductive abilities, but also as a possible mechanism for staving off the effects of aging.

Authors' contributions: EGS and MAS: Study concept and design; acquisition of data; analysis and interpretation of data. RPA, LSG, DSS and WAO: Performed experiments. LTR: Critical revision of the manuscript for important intellectual content. RLP: Study concept and design; supervision.

ACKNOWLEDGMENTS

We would like to thank Dr. Tiago da Silveira Vasconcelos for the critical reading of the manuscript. We also thank all the members of the Molecular Biology and Cytogenetics Laboratory of Sagrado Coração University (USC) for their assistance, their stimulating discussions, and the reagents.

DECLARATION OF CONFLICTING INTERESTS

The author(s) declared no potential conflicts of interest with respect to the research, authorship, and/or publication of this article.

FUNDING

The author(s) disclosed receipt of the following financial support for the research, authorship, and/or publication of this article: Work in our laboratory has been supported by the São Paulo Research Foundation (FAPESP) under grant numbers 2012/22009-7; 2016/04580-0; 2018/01554-3.

REFERENCES

1. Organization WH. *Resumo relatório mundial de envelhecimento e saúde*. Genebra: World Health Organization, 2015, p.28
2. Nations U. Development in an ageing world. In: *world economic and social survey*. New York: United Nations, 2007, p.180
3. Lopez-Otin C, Blasco MA, Partridge L, Serrano M, Kroemer G. The hallmarks of aging. *Cell* 2013;**153**:1194–217
4. Grammatikakis I, Panda AC, Abdelmohsen K, Gorospe M. Long noncoding RNAs(lncRNAs) and the molecular hallmarks of aging. *Aging* 2014;**6**:992–1009
5. Kim J, Kim KM, Noh JH, Yoon JH, Abdelmohsen K, Gorospe M. Long noncoding RNAs in diseases of aging. *Biochim Biophys Acta* 2016;**1859**:209–21
6. Brooks RC, Garratt MG. Life history evolution, reproduction, and the origins of sex-dependent aging and longevity. *Ann N Y Acad Sci* 2017;**1389**:92–107
7. Orozco-Solis R, Sassone-Corsi P. Circadian clock: linking epigenetics to aging. *Curr Opin Genet Dev* 2014;**26**:66–72
8. Angelopoulou R, Lavranos G, Manolakou P, Katsiki E. Fertility in the aging male: molecular pathways in the anthropology of aging. *Coll Antropol* 2013;**37**:657–61
9. Head JR, Kresge CK. Reaction of the chromatoid body with a monoclonal antibody to a rat histocompatibility antigen. *Biol Reprod* 1985;**33**:1001–8
10. Chuma S, Hosokawa M, Kitamura K, Kasai S, Fujioka M, Hiyoshi M, Takamune K, Noce T, Nakatsuji N. Tdrd1/Mtr-1, a tudor-related gene, is essential for male germ-cell differentiation and nuage/germinal granule formation in mice. *Proc Natl Acad Sci U S A* 2006;**103**:15894–9
11. Deng W, Lin H. miwi, a murine homolog of piwi, encodes a cytoplasmic protein essential for spermatogenesis. *Dev Cell* 2002;**2**:819–30
12. Toyooka Y, Tsunekawa N, Takahashi Y, Matsui Y, Satoh M, Noce T. Expression and intracellular localization of mouse Vasa-homologue protein during germ cell development. *Mech Dev* 2000;**93**:139–49
13. Kotaja N, Sassone-Corsi P. The chromatoid body: a germ-cell-specific RNA-processing centre. *Nat Rev Mol Cell Biol* 2007;**8**:85–90
14. Meikar O, Da Ros M, Korhonen H, Kotaja N. Chromatoid body and small RNAs in male germ cells. *Reproduction* 2011;**142**:195–209
15. Meikar O, Da Ros M, Kotaja N. Epigenetic regulation of male germ cell differentiation. *Subcell Biochem* 2013;**61**:119–38
16. Yadav RP, Kotaja N. Small RNAs in spermatogenesis. *Mol Cell Endocrinol* 2014;**382**:498–508
17. Peruquetti RL. Perspectives on mammalian chromatoid body research. *Anim Reprod Sci* 2015;**159**:8–16
18. Meikar O, Vagin VV, Chalmel F, Sostar K, Lardenois A, Hammell M, Jin Y, Da Ros M, Wasik KA, Toppari J, Hannon GJ, Kotaja N. An atlas of chromatoid body components. *RNA* 2014;**20**:483–95
19. Peruquetti RL, de Mateo S, Sassone-Corsi P. Circadian proteins CLOCK and BMAL1 in the chromatoid body, a RNA processing granule of male germ cells. *PLoS One* 2012;**7**:e42695
20. Schoeller EL, Clark DD, Dey S, Cao NV, Semaan SJ, Chao LW, Kauffan AS, Stowers L, Mellon PL. Bmal1 is required for normal reproductive behaviors in male mice. *Endocrinology* 2016;**157**:2–28
21. Animal CNdCdE. Resolução Normativa CONCEA no 13, de 20.09.2013. In: *Normativas do CONCEA para produção, manutenção ou utilização de animais em atividades de ensino ou pesquisa científica*. Brasília: Ministério da Ciência, Tecnologia e Inovação (MCTI), 2015, p.328
22. Robb GW, Amann RP, Killian GJ. Daily sperm production and epididymal sperm reserves of pubertal and adult rats. *J Reprod Fertil* 1978;**54**:103–7
23. Garcia PV, Arroteia KF, Joazeiro PP, Mesquita SFP, Kempinas WG, Pereira LAV. Orchidopexy restores morphometric-stereologic changes in the caput epididymis and daily sperm production in cryptorchidic mice, although sperm transit time and fertility parameters remain impaired. *Fertil Steril* 2011;**96**:6
24. Bjorndahl L, Soderlund I, Kvist U. Evaluation of the one-step eosin-nigrosin staining technique for human sperm vitality assessment. *Hum Reprod* 2003;**18**:813–6
25. Kotaja N, Kimmins S, Brancorsini S, Hentsch D, Vonesch JL, Davidson I, Parvinen M, Sassone-Corsi P. Preparation, isolation and characterization of stage-specific spermatogenic cells for cellular and molecular analysis. *Nat Meth* 2004;**1**:249–54
26. Zar JH. *Biostatiscical analysis*. 4th ed. New Jersey: Prentice Hall, 1999
27. Gunes S, Hekim GN, Arslan MA, Asci R. Effects of aging on the male reproductive system. *J Assist Reprod Genet* 2016;**33**:441–54
28. Machida T, Yonezawa Y, Noumura T. Age-associated changes in plasma testosterone levels in male mice and their relation to social dominance or subordinance. *Horm Behav* 1981;**15**:238–45
29. Bae J, Choi H, Choi Y, Roh J. Dose- and time-related effects of caffeine on the testis in immature male rats. *Exp Anim* 2017;**66**:29–39
30. Alvarez JD, Hansen A, Ord T, Bebas P, Chappell PE, Giebultowicz JM, Williams C, Moss S, Sehgal A. The circadian clock protein BMAL1 is necessary for fertility and proper testosterone production in mice. *J Biol Rhythms* 2008;**23**:26–36
31. Parvinen M. The chromatoid body in spermatogenesis. *Int J Androl* 2005;**28**:189–201
32. Yokota S. Nuage proteins: their localization in subcellular structures of spermatogenic cells as revealed by immunoelectron microscopy. *Histochem Cell Biol* 2012;**138**:1–11
33. de Mateo S, Sassone-Corsi P. Regulation of spermatogenesis by small non-coding RNAs: role of the germ granule. *Semin Cell Dev Biol* 2014;**29**:84–92

34. Haraguchi CM, Mabuchi T, Hirata S, Shoda T, Hoshi K, Akasaki K, Yokota S. Chromatoid 35 bodies: aggresome-like characteristics and degradation sites for organelles of spermiogenic cells. *J Histochem Cytochem* 2005;**53**(4):455–65.
35. Kotaja N, Bhattacharyya SN, Jaskiewicz L, Kimmins S, Parvinen M, Filipowicz W, 30 Sassone-Corsi P. The chromatoid body of male germ cells: similarity with processing bodies and presence of Dicer and microRNA pathway components. *Proc Natl Acad Sci U S A* 2006;**103**(8):2647–52.
36. Woodland HR. The birth of animal development: multicellularity and the germline. *Curr Top Dev Biol* 2016;**117**:609–30
37. Woodland HR. The birth of animal development: multicellularity and the germline. *Curr Top Dev Biol* 2016;**117**:609–30.
38. Mori MA, Raghavan P, Thomou T, Boucher J, Robida-Stubbs S, Macotela Y, Russell SJ, Kirkland JL, Blackwell TK, Kahn CR. Role of microRNA processing in adipose tissue in stress defense and longevity. *Cell Metab* 2012;**16**(3):336–47.
39. Amigo I, Meezes-Filho SL, Luevano-Martinez LA, Chausse B, Kowaltowski AJ. Caloric restriction increases brain mitochondrial calcium retention capacity and protects against excitotoxicity. *Aging Cell* 2017;**16**(1):73–81.

(Received January 20, 2018, Accepted May 30, 2018)